Supplementary Information

Three-dimensional patterning of MoS_2 with ultrafast laser

Dezhi Zhu†, Ming Qiao†, Jianfeng Yan*, Jiawang Xie, Heng Guo, Shengfa Deng, Guangzhi He, Yuzhi Zhao, Ma Luo

State Key Laboratory of Tribology in Advanced Equipment, Department of Mechanical Engineering, Tsinghua University, Beijing 100084 China.

* Corresponding author: yanjianfeng@tsinghua.edu.cn

† These authors contributed equally to this work.

Plasma model combined with two temperature model

Because the bandgap of bulk MoS_2, 1.8 eV, is higher than the photon energy, 1.5 eV, double-photon ionization is considered as the main method to generate free electrons. The following plasma equation is applied to calculate the free electron generation:[1,2]

$$\frac{\partial n_f}{\partial t} = P(I) - \frac{n_f}{\tau_{re}} \tag{1}$$

where n_f is the free electron density, t is the time, τ_{re} is the free electron recombination time, $P(I)$ is the photoionization term, and I is the laser intensity. The free electron recombination time τ_{re} is considered a constant value at 180 ps, as measured for MoS_2 in a previous work.[3] The photoionization term can be calculated by formula for double-photon absorption as follows:[4]

$$P = \frac{\beta I^2}{2\hbar\omega} \tag{2}$$

$$I = \frac{2F}{\sqrt{\pi/ln2}t_p}(1-R) \times exp\left(-\frac{r^2}{r_0} - (4ln2)\left(\frac{t}{t_p}\right)^2 - \int_0^z \alpha_h(t,r,z)dz\right) \tag{3}$$

where $\hbar$ is the reduced Planck constant, and ω is the laser frequency, F is the laser fluence, t_p is the pulse duration, r_0 is the radius of the laser beam, α_h is the free electron absorption coefficient.

Meanwhile, the ionized free electrons are also heated by an intense electromagnetic field during laser irradiation. The electron temperature during laser irradiation can be calculated using the following expression:[2]

$$c_e n_f \frac{\partial T_e}{\partial t} = \alpha_h I \tag{4}$$

where c_e is the specific heat of free electrons, T_e is the free electron temperature, which can be deduced from the free electron dielectric function. The specific heat of the free electrons can be deduced from the Fermi distribution.[5]

Based on eqs. 1–4, we can obtain the values of free electron density and temperature after laser pulse excitation. In this case, the energy of the laser pulse is transferred to the high energy free electron system. Subsequently, the high energy free electrons transfer energy to lattice and valence electrons through high energy electron induced lattice heating and valence electron ionization.

To describe lattice heating, the famous two-temperature model (TTM) was used to calculate the energy transfer between high energy electrons and lattice as follows: [5,6]

$$c_e \frac{\partial T_e}{\partial t} = \nabla[\kappa_e \nabla T_e] - G(T_e - T_l) + S \tag{5}$$

$$c_l \frac{\partial T_l}{\partial t} = G(T_e - T_l) \tag{6}$$

where κ_e is the free electron heat conductivity, G is the electron-lattice coupling factor, T_l is the temperature of the lattice, S is the laser source term, and c_l is the specific heat of the lattice. Because the processes of lattice heating and laser excitation were separated in time domains, the laser source term, S, was ignored in the simulation presented in eq. 5. The free electron heat conductivity can be

obtained as 4.2 cm^2/s from experimental measurements.[5] The electron-lattice coupling factor can be estimated using the following:[5,7]

$$G = \frac{\pi^2 m_e n_f {c_s}^2}{6\tau_{el} T_e} \tag{7}$$

where m_e is the mass of the electron, c_s is the sound speed in MoS_2, and τ_{el} is the free electron relaxation time. The sound speed can be obtained using $c_s = \sqrt{B/\rho}$, where B is the bulk modulus (B=2.4e^{12} Nm^{-2}), and ρ is the mass density of MoS_2 (ρ=4.8 gcm^{-3}). The specific heat of the lattice can be deduced from the Debye model.[4]

In a previous work on the laser induced superheat of a semiconductor, the plasma frequency ω_p was reported to increase with lattice temperature as follows:[8]

$${\omega_p}^{-1} \frac{\partial \omega_p}{\partial T_l} = K_c \tag{8}$$

where K_c=8.2e^{-4}, and the plasma frequency ω_p is a function of the free electron density n_f:[1,8]

$${\omega_p}^2 = \frac{n_f e^2}{m_e \varepsilon_0} \tag{9}$$

where ε_0 is the vacuum dielectric constant (ε_0=3.915+3.166i). Based on eqs. 8–9, we can obtain the relationship between free electron density and lattice temperature. Therefore, the electron density evolution can be calculated after laser pulse excitation.

The transient optical property can be described as the dielectric function of laser induced plasma. There are mainly two contributions to the dielectric function for semiconductors (*e.g.*, free electrons and valence electrons). In some previous works,[9,10] the dielectric function change was only determined

by the effect of free electrons, where the contribution of free electrons to the dielectric function is widely described by the Drude-Lorentz model.[1] For transparent material, the contribution of valence electrons is so small that it can be ignored. However, the effect of valence electrons on the dielectric function should be taken into account, especially when valence electron density considerably decreases because of strong ionization. Therefore, to determine the contribution of valence electrons, the dielectric function should be expressed as follows:[11]

$$\varepsilon = \left(1 + \frac{3(n_0 - n_f)\chi}{3 - (n_0 - n_f)\chi}\right) - \frac{{\omega_p}^2}{\omega^2 + i\omega\Gamma} \tag{10}$$

where ε is the dielectric function, n_0 is the original valence electron density in bulk MoS_2, ω is the laser frequency, χ is the electric susceptibility derived from the Clausius–Mossotti relation (χ=0.9672+0.1114i), and Γ is the free electron scattering rate.[1] The free electron scattering rate is attributed to the effect of electron-lattice scattering and electron-electron scattering.[4] When the dielectric function is determined, the time-resolved reflection can be calculated in the laser irradiated area as follows:[12]

$$R = \frac{(n-1)^2 + \kappa^2}{(n+1)^2 + \kappa^2} \tag{11}$$

where n and κ are the refraction index and the extinction coefficient, respectively, which can be deduced from the dielectric function by $n + i\kappa = \sqrt{\varepsilon}$.

Based on the discussion aforementioned, we combined plasma and two temperature model to account for the electron dynamics of MoS_2 during intense femtosecond laser pulse irradiation. The simulation results were analyzed and compared with the experimental results.

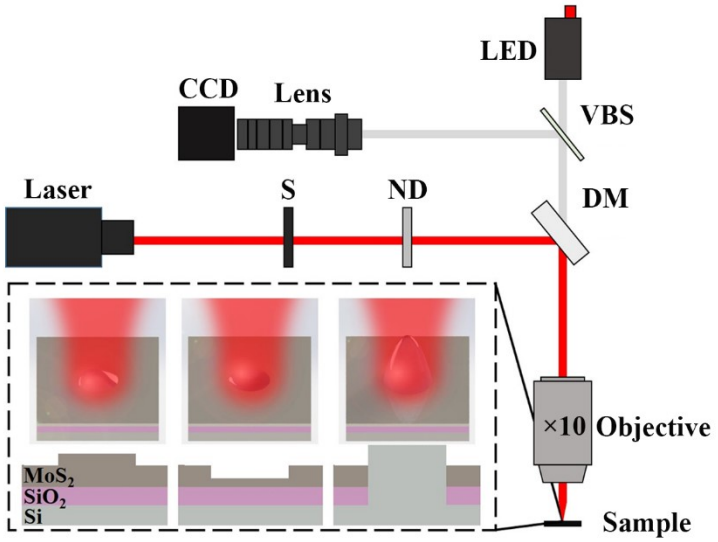

Figure S1. Schematic illustration of experimental setup for processing MoS_2 using a femtosecond laser.

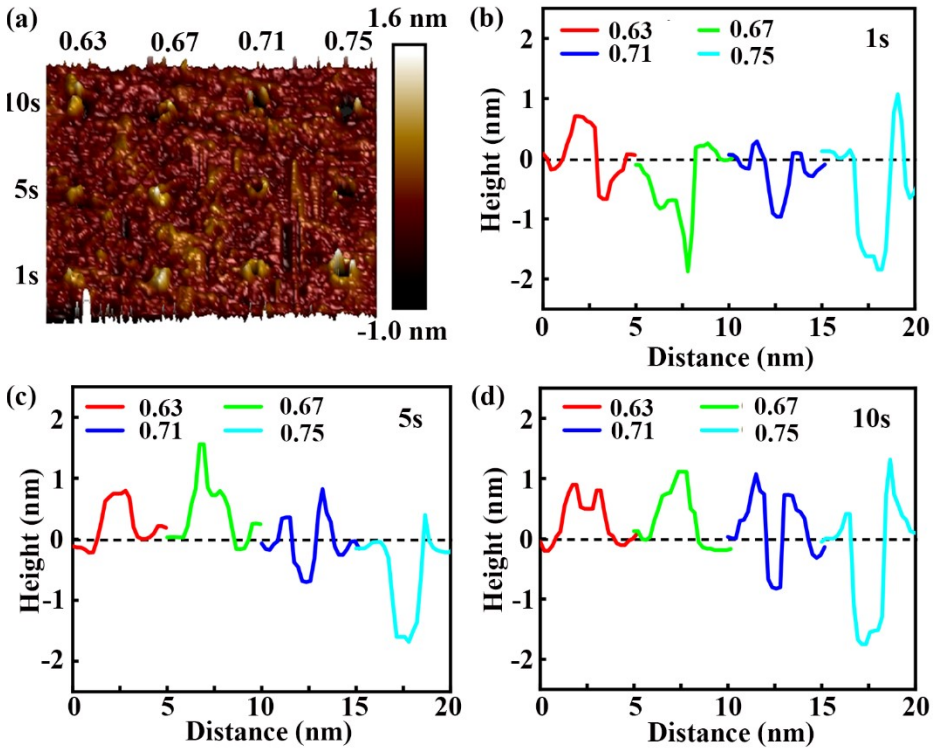

Figure S2. Surface morphologies of point processing. (a) AFM topography of points ablated using ultrafast laser with different fluence and time. AFM height images of points ablated using ultrafast laser with (b) 1s, (c) 5s and (d) 10s.

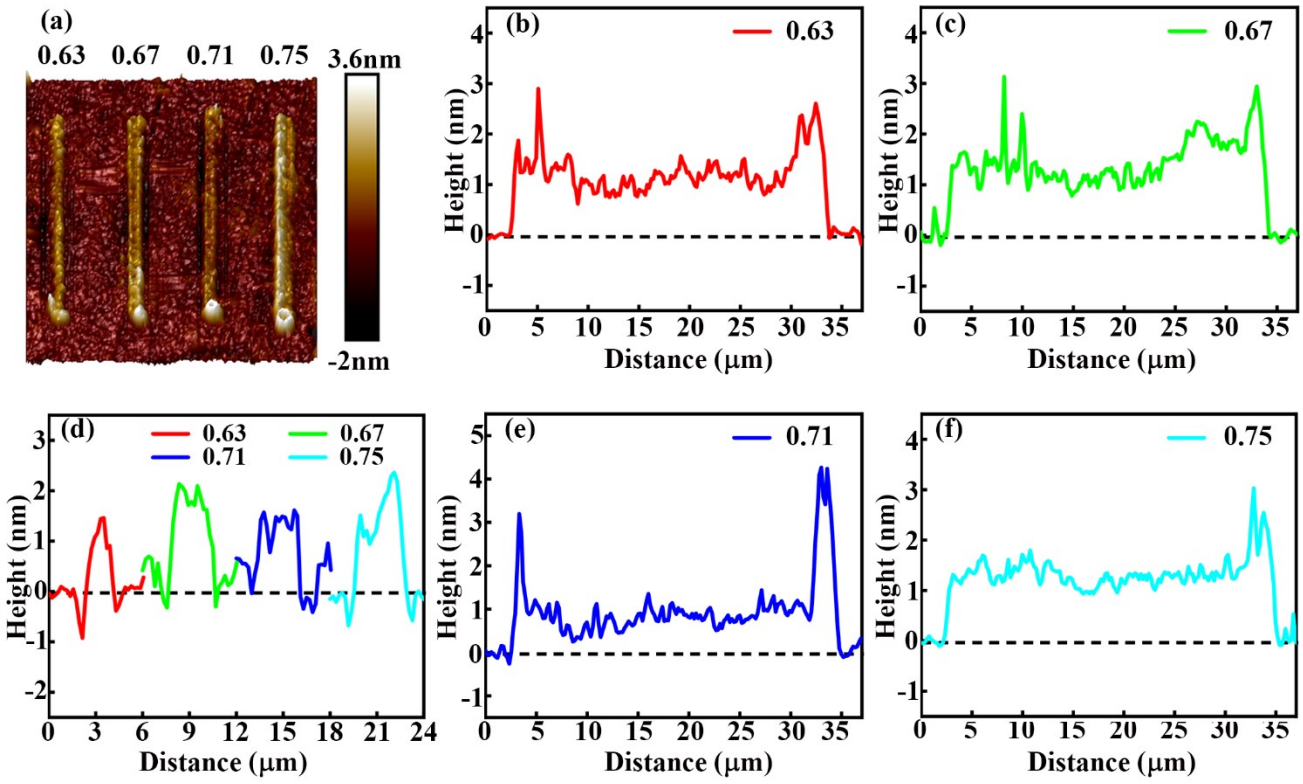

Figure S3. Surface morphologies of line processing. (a) AFM topography of line ablated using ultrafast laser with different fluence. AFM height images of lines ablated using ultrafast laser with (b) 0.63 J/cm^2, (c) 0.67 J/cm^2, (e) 0.71 J/cm^2 and (f) 0.75 J/cm^2. (d) The AFM height comparison ablated using ultrafast laser with different fluence.

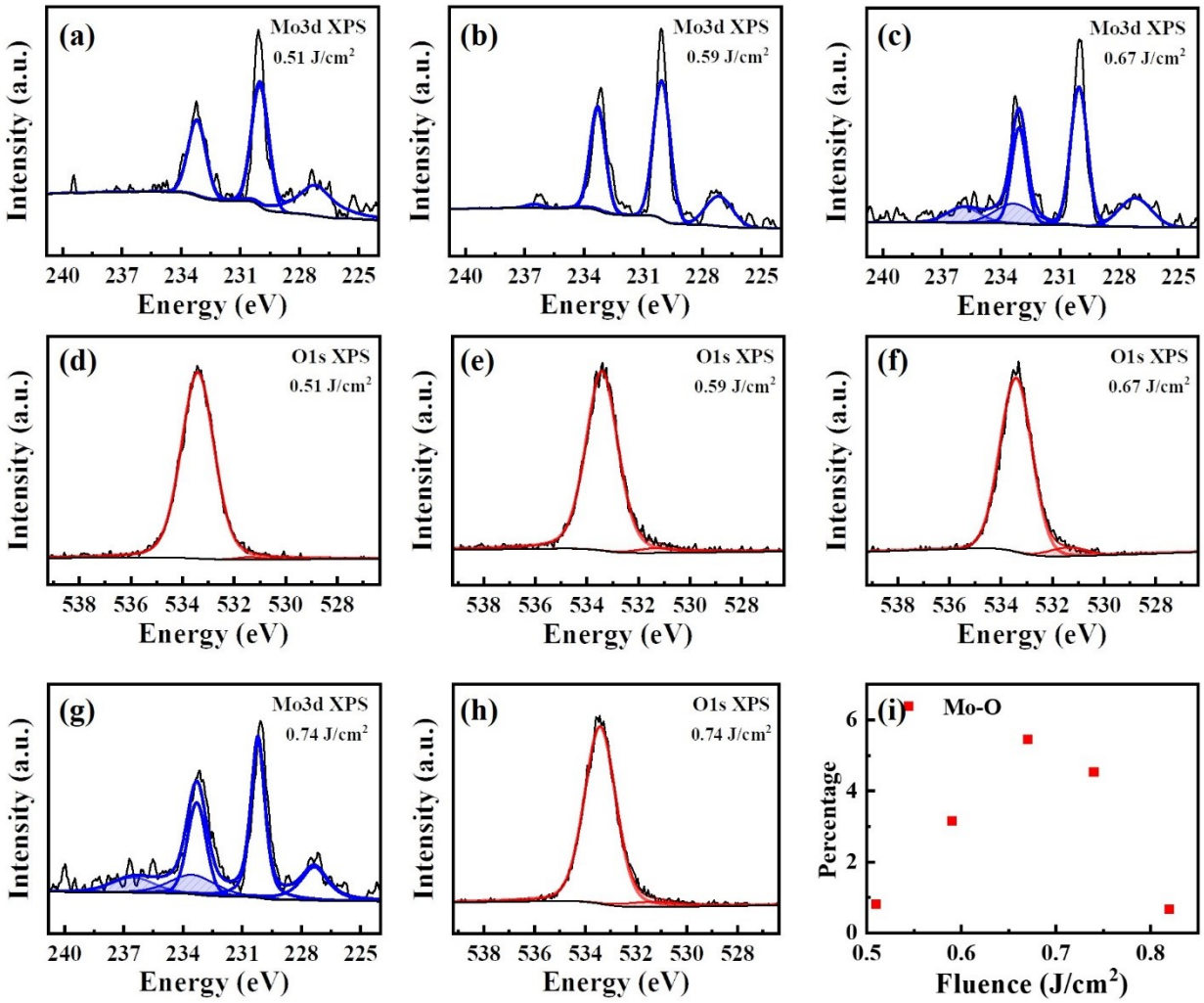

Figure S4. XPS spectrum of oxygen and molybdenum in MoS_2 after laser patterning with different fluence.

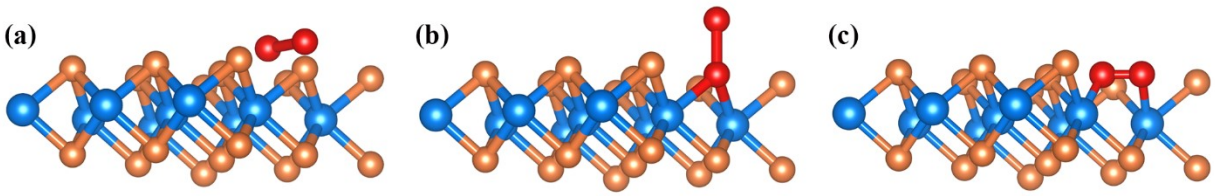

Figure S5. Crystal structures for (a) Configuration II, (b) Configuration III, (c) Configuration IV.

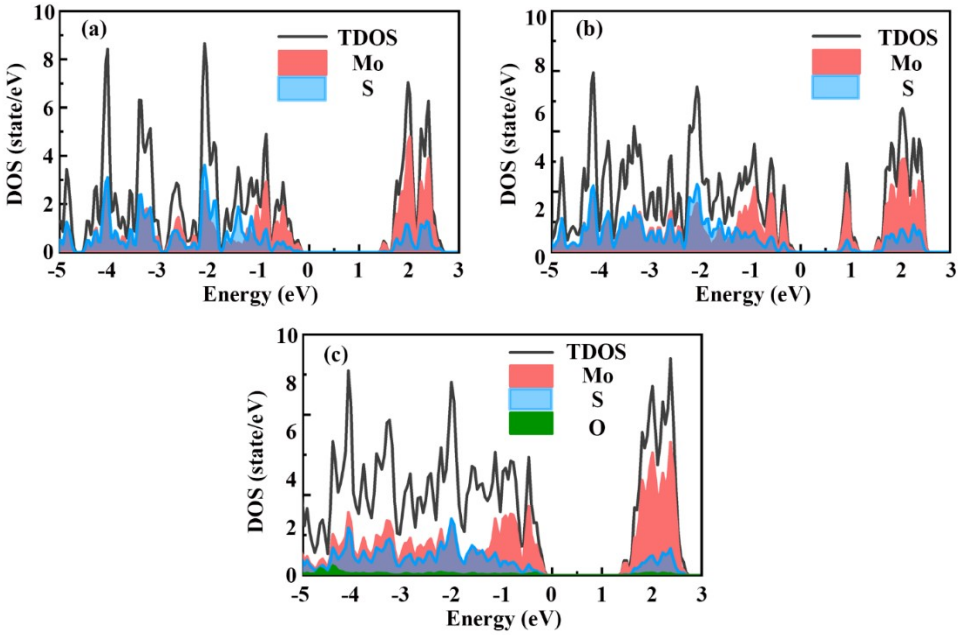

Figure S6. Electronic density of states obtained through DFT of (a) pristine MoS_2, (b) MoS_2 with S vacancies, (c) MoS_2 with O substituting S. Zero at the energy scale corresponds to the Fermi level.

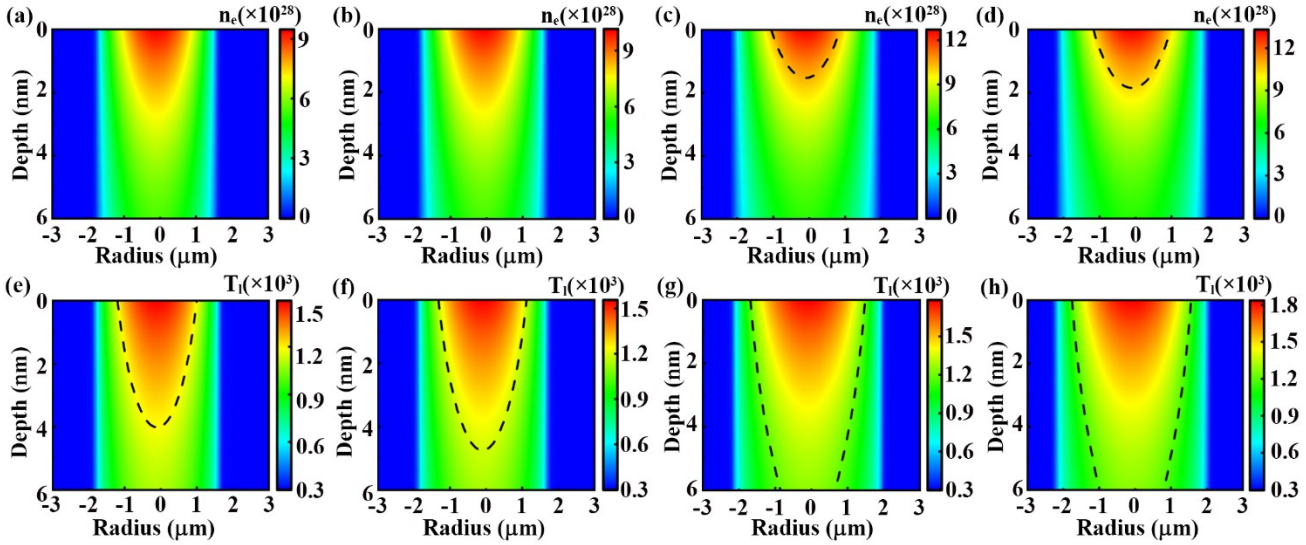

Figure S7. Calculated electron densities ablated by femtosecond laser pulse with different fluence of (a) 0.64, (b) 0.66, and (c) 0.74 J/cm^2 and (d) 0.76 J/cm^2. Calculated temperature distributions ablated by femtosecond laser pulse with different fluence of (e) 0.64, (f) 0.66, and (g) 0.74 J/cm^2 and (h) 0.76 J/cm^2.

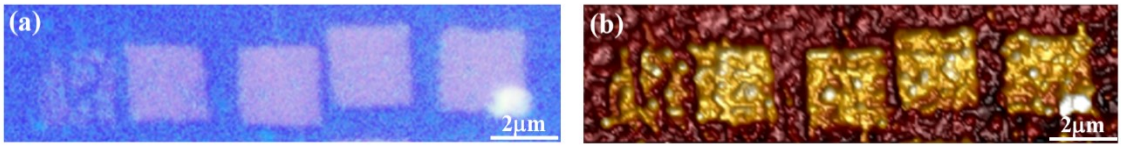

Figure S8. The optical image and AFM topography of square patterns using ultrafast laser with different fluence from 0.58~0.68 J/cm^2.

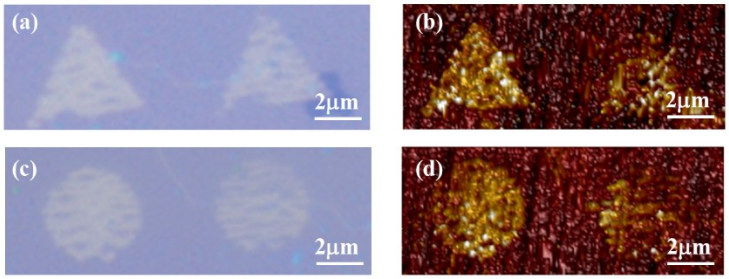

Figure S9. The optical image and AFM topography of (a, b) triangle and (c, d) circle patterns using ultrafast laser with different fluence from 0.58~0.68 J/cm^2.

References

[1] P. Balling and J. Schou, *Rep Prog Phys*, **2013**, 76, 036502.

[2] L. Jiang and H.-L. Tsai, *J. Heat Transfer*, **2005**, 127, 1167.

[3] N. Kumar, J. He, D. He, Y. Wang and H. Zhao, *J. Appl. Phys.*, **2013**, 113.

[4] L. Jiang and H. L. Tsai, *Int. J. Heat Mass Transfer*, **2005**, 48, 487-499.

[5] L. Jiang and H.-L. Tsai, *J. Appl. Phys.*, **2008**, 104.

[6] C. W. Cheng, S. Y. Wang, K. P. Chang and J. K. Chen, *Appl. Surf. Sci.*, **2016**, 361, 41-48.

[7] T. Shin, S. W. Teitelbaum, J. Wolfson, M. Kandyla and K. A. Nelson, *The Journal of Chemical Physics*, **2015**, 143, 194705.

[8] J. Boneberg, O. Yavas, B. Mierswa and P. Leiderer, *Phys. Status Solidi. B*, **1992**, 174, 295-300.

[9] P. K. Velpula, M. K. Bhuyan, F. Courvoisier, H. Zhang, J. P. Colombier and R. Stoian, *Laser Photonics Rev.*, **2016**, 10, 230-244.

[10] Q. Sun, H. Jiang, Y. Liu, Z. Wu, H. Yang and Q. Gong, *Opt. Lett.*, **2005**, 30, 320-322.

[11] S. Guizard, A. Semerok, J. Gaudin, M. Hashida, P. Martin and F. Quéré, *Appl. Surf. Sci.*, **2002**, 186, 364-368.

[12] R. Gunnella, G. Zgrablic, E. Giangrisostomi, F. D'Amico, E. Principi, C. Masciovecchio, A. Di Cicco and F. Parmigiani, *Phys. Rev. B*, **2016**, 94.